Relationship between mega-scale glacial lineations and iceberg ploughmarks on the Bjørnøyrenna Palaeo-Ice Stream bed, Barents Sea

Emilia D. Piasecka[1], Chris R. Stokes[2], Monica C.M. Winsborrow[1*], Karin Andreassen[1]

(1) Centre for Arctic Gas Hydrates, Environment and Climate (CAGE) , Department of Geosciences, UiT The Arctic University of Norway, Tromsø, Norway

(2) Department of Geography, Durham University, UK

*corresponding author: monica.winsborrow@uit.no

Keywords: Glacial geomorphology; Mega-scale glacial lineations; Groove-ploughing; Bjørnøyrenna Palaeo-Ice Stream; Barents Sea Ice Sheet

Abstract

Mega-scale glacial lineations (MSGLs) are ridge-groove corrugations aligned in the direction of the former ice flow, tens of kilometers long and up to a few hundreds meters wide. They are the most striking subglacial features on the beds of former ice streams and play an important role in modulating ice flow through their influence on bed roughness and subglacial hydrology. Despite the importance of MSGLs, their formation remains enigmatic. Most studies have tended to focus on assemblages of MSGLs and their relationship to other landforms up-ice (e.g. drumlins or bedrock features in ice stream onset zones) but fewer studies have examined their characteristics and transition to other landforms towards ice stream grounding lines. In this paper we investigate the relationship between an assemblage of MSGLs and ploughmarks on the bed of the former Bjørnøyrenna Ice Stream in the SW Barents Sea, which

25 occurs in the central part of the ice stream bed. A sample of MSGLs is used to test their potential
26 origin, based on their metrics (width, length) and diagnostic characteristics predicted by
27 formation theories. Results show a down-flow depth decrease of the MSGL grooves, and a
28 shallowing tendency once they transition into ploughmarks. Their width shows an increasing
29 tendency, which we link mostly to the strong divergence of the trough (and ice flow)
30 downstream. The prominent continuity from linear to curvilinear features demonstrates that the
31 grooves associated with MSGLs transition into iceberg ploughmarks. This observation is
32 consistent with the hypothesis that the MSGLs have formed through a mechanism of 'groove-
33 ploughing', at least in part. The continuity from MSGLs to iceberg ploughmarks resulted from
34 detachment of large icebergs from the grounded ice wall or grounded ice shelf and their
35 ploughing away from the ice margin.

1. Introduction

Fast flowing-ice streams are key components of an ice sheet and exert an important influence on their mass balance and geometry. In Antarctica, for example, they are thought to be responsible for about 90% of the overall ice discharge (Bentley and Giovinetto, 1991; Bamber et al., 2000; Bennett, 2003) and they are known to have played an important role in palaeo-ice sheet mass balance (Stokes and Clark, 2001; Ottesen et al., 2005; Stokes et al., 2016; Robel and Tziperman, 2016). The coupling between an ice stream base and the underlying sediments exerts a fundamental control on ice stream dynamics (Bell et al., 1998; Bennett, 2003; Clark et al., 2003; Smith and Murray, 2009; Stokes, in press). Basal traction (including shearing between subglacial sediment and the ice stream base, and form drag due to obstacles at the ice stream bed) is critical for regulating the velocity and trajectory of ice stream flow (Benn and Evans, 2010; Stokes et al., 2007; Tulaczyk et al., 2000; Winsborrow et al., 2016). A principal landform on the beds of former (e.g. Clark, 1993; Stokes et al., 2013; Spagnolo et al., 2014; Spagnolo et al., 2016) and contemporary ice streams (King et al., 2009) are mega-scale glacial lineations (MSGLs), which are considered a diagnostic signature of fast-flowing ice (Clark, 1993).

MSGLs are elongated ridge-groove furrows aligned in the direction of ice-flow. They are often several kilometers long, 200-300 m wide, and have amplitudes of 1 to 10 m (Spagnolo et al., 2014), although more extreme values exist. For example, at the modern Rutford Ice Stream bed, the peak-to-trough amplitude of MSGLs is up to 90 m (King et al., 2009), but the mean value (10 m) is more consistent with the palaeo-record (Spagnolo et al., 2014). The mechanisms of MSGLs formation remain debated and there are several hypotheses to explain their formation (Clark et al., 2003; Shaw et al., 2008; King et al., 2009; Fowler, 2010; Stokes et al., 2013; Spagnolo et al., 2014; Spagnolo et al., 2016). Important to this debate is whether MSGLs are constructional landforms that are somehow built up, elongated and accreted (Spagnolo et al.,

2016), or whether they are formed by both depositional and erosional processes, where the material from within grooves is being excavated, leaving MSGLs on either side (e.g. Clark, 1993). Clark (1993) proposed a 'groove-ploughing' hypothesis that explained MSGLs as the product of basal ice keels that plough through soft sediments, like a 'garden rake' ploughs soil. Only a handful of studies have tested this hypothesis (although see Stokes et al., 2013; Spagnolo et al., 2014; Spagnolo et al., 2016), but a prediction would be that once the keels cross the ice stream grounding line, they would continue as iceberg-ploughmarks (Clark et al., 2003). Perhaps surprisingly, therefore, very few studies have examined the morphological relationship between MSGLs and iceberg ploughmarks in the vicinity of ice stream grounding zones, which might offer a useful test of this and other formation theories. In this paper we present a striking suite of MSGLs from the bed of Bjørnøyrenna Palaeo-Ice Stream and document clear evidence of a continuous transition from MSGL grooves to iceberg ploughmarks. This continuity is consistent with the notion that these MSGLs were formed through groove-ploughing.

1.1. Previous work on mega-scale glacial lineations (MSGLs)

MSGLs were first identified on Landsat images in Canada, and were initially thought to be a separate group of bedforms, much larger in length than drumlins or megaflutes (Clark, 1993), although more recent work suggest they lie at one end of a bedform continuum (Ely et al., 2016). This continuum is directly related to ice velocity and also includes ribbed moraines and drumlins (Aario, 1977a; Ely et al., 2016). MSGLs typically display a spatial coherency within particular ice-flow assemblages, such as their exceptional parallel alignment (similar orientation), close proximity and relatively even spacing, and similar morphometry (Clark, 1993, 1999; Spagnolo et al., 2014; 2016).

The size and shape of MSGLs, such as their length, relief and orientation, have been used for various interpretations regarding ice stream trajectory, relative ice velocity, erosional

potential and sediment transport (Clark, 1993; Jakobsson et al., 2012a; Ó Cofaigh et al., 2013; Stokes et al., 2013; Spagnolo et al., 2014; Barchyn et al., 2016; Spagnolo et al., 2016). Assemblages of MSGLs revealed on exposed beds of former ice streams also provide insight into their past dynamics and can contribute to our understanding of future changes in contemporary ice streams (Holt et al., 2006; Nitsche et al., 2013; Margold et al., 2015; Patton et al., 2015; Stokes et al., 2016).

Many examples of MSGLs have been identified on the beds of palaeo-ice streams (e.g. Clark, 1993; Ottesen et al., 2005; Dowdeswell et al., 2010; Hogan et al., 2010; Winsborrow et al., 2010; Livingstone et al., 2012; Stokes et al., 2013; Bjarnadóttir et al., 2014; Spagnolo et al., 2014), yet their origin remains unclear (Clark, 1993; Clark et al., 2003; Fowler, 2010; Ó Cofaigh et al., 2010). Given the widespread association of MSGLs and rapid ice flow, understanding the processes which contribute to their formation would represent a significant advance in our understanding and ability to model subglacial processes and erosional potential of ice streams (Stokes, in press). The largely undisturbed, marine-based Bjørnøyrenna Palaeo-Ice Stream bed, represents an ideal location to study processes of MSGLs formation and can be used as a tool to understand modern ice streams in Antarctica and Greenland (Andreassen et al., 2014; Patton et al., 2016).

1.2. Formational theories

Several theories for MSGLs formation have been proposed, including subglacial till deformation (Clark, 1993), groove-ploughing (Clark et al., 2003), erosion by subglacial floods (Shaw et al., 2008), and a flow instability of subglacial meltwater that relates to the formation of rills (Fowler, 2010).

Clark (1993) was the first to formally identify and name MSGLs, and proposed their formation mechanism to be similar to that forming other ice-moulded landforms, such as

drumlins (cf. Boulton and Hindmarsh, 1987). His initial ideas suggested that MSGLs might form as a result of fast-flowing ice, deforming and eroding sediments subglacially in a streamlined manner, similar to that proposed to explain drumlin formation (Boulton and Hindmarsh, 1987). The initiation of the deformation was suggested to occur around substrate irregularities, with ice-flow velocities and duration of the flow as controlling factors (Clark, 1993). Therefore, MSGLs would be part of a subglacial bedform continuum, and according to this theory may likely evolve from attenuation and deformation of drumlins, under high strain rates and high sediment supply (Clark, 1993; Stokes et al., 2013).

The groove-ploughing mechanism of formation (Tulaczyk et al., 2001; Clark et al., 2003) suggests that these landforms are dependent on the presence of longitudinally oriented irregularities at the ice stream base (keels), which form as the ice stream passes over a rough bed upstream or through lateral compression of the ice stream. These protuberances at the ice stream base will be further amplified as the ice stream converges (Tulaczyk et al., 2001; Clark et al., 2003). The keels will plough through the underlying sediments, producing a grooved surface, as the ice stream moves over the weaker till. The theory perceives MSGLs as mainly erosional features, with the neighbouring ridges being a by-product of the ploughing of the keel (Clark et al., 2003; Ó Cofaigh et al., 2005).

The groove-ploughing hypothesis makes predictions related to MSGL morphology and the nature of their occurrence. One prediction is that there will be a downstream decrease in the depth of the MSGLs grooves, due to melting of the keels at the ice stream base as they plough sediments. Depending on the properties of ice and/or the weakness of sediments, the reduction in groove-depth might be considerable or minimal (Clark et al., 2003). The theory further predicts that MSGLs should be located downstream from areas where basal keels are produced (e.g. strong convergence zone or bedrock features). Another important factor for the generation of ice keels is the roughness at the ice stream base, which should be greater across the ice stream

than along the flowline. Lastly, the grooves at the inferred grounding line and downstream from there may display certain sinuosity and changes in direction, as the ungrounded ice will be laterally much less stable (Clark et al., 2003). As noted above, these predictions have rarely been tested explicitly, although qualitative arguments have been proposed that both support (Tulaczyk et al., 2001; Stokes and Clark, 2003; Ó Cofaigh et al., 2005; Ó Cofaigh et al., 2013) or refute the theory (King et al., 2009; Spagnolo et al., 2016). In some case studies, authors have concluded that groove-ploughing may be just one of the processes involved in their generation, often suggested to modify existing lineations, rather than creating them (e.g. Ó Cofaigh et al., 2002; Ó Cofaigh et al., 2005; King et al., 2009; Stokes et al., 2013). The main evidence against groove ploughing is that MSGLs have in some cases been observed to initiate within grooves (King et al., 2009; Stokes et al., 2013), bifurcate, merge, or occur in areas distant from any upstream bedrock structures that may have shaped the ice base (Ó Cofaigh et al., 2005). Some measurements of their width have also revealed a regularity along flow (Clark, 1993; Stokes et al., 2013), but sometimes the width increases downstream (Ó Cofaigh et al., 2005), contrary to predictions. Amplitude increases have also been observed in a number of cases (Ó Cofaigh et al., 2005). Thus, most of the empirical studies involving MSGLs morphology and their formation point to groove-ploughing as a transient and localised process (Ó Cofaigh et al., 2002; Ó Cofaigh et al., 2005; Ó Cofaigh et al., 2013; Stokes et al., 2013).

The meltwater flood theory (Shaw, 1983; Shaw et al., 2008; Shaw and Sharpe, 1987) is, perhaps, most controversial and suggests that a range of subglacial bedforms including MSGLs, relate to discharge of catastrophic amounts of turbulent subglacial meltwater. This theory envisages subglacial bedform generation by infilling of subglacial cavities and/or erosion of inter-bedform areas. This theory has been questioned for a number of reasons, not least because of the large volumes of water that are required (Clarke et al., 2005), but also from observations of flutings on modern glacier forelands (Evans and Twigg, 2002), and drumlins and MSGLs

161 actively forming beneath contemporary ice streams (Smith et al., 2007; King et al., 2009) in the
162 absence of large subglacial meltwater discharges.

163 More recently, a rilling instability theory has been proposed (Fowler, 2010), based on
164 mathematical modelling of the subglacial hydrological system. The theory suggests that
165 meltwater at the ice-bed interface is unstable and organizes into several narrow streams (rills),
166 eroding grooves separated by ridges. Model simulations were able to produce longitudinal
167 'rolls' aligned in ice flow direction, with modelled dimensions (length 52.9 km, width 394 m)
168 of the same order of magnitude as some empirical MSGLs observations (e.g. Clark, 1993;
169 Andreassen and Winsborrow, 2009; Piasecka et al., 2016). However, the range of MSGL
170 dimensions reported in literature is large (lengths from <1 km (Graham et al., 2009;
171 Winsborrow et al., 2012) up to 180 km (Andreassen et al., 2007; Andreassen et al., 2008) and
172 widths from <40 m (Stokes et al., 2013) up to 5 km (Andreassen et al., 2007), and the modelled
173 values are highly dependent on particular parameters chosen for the experiment.

174 In addition to the rilling theory, it has been proposed that of spiral flows in basal ice (Shaw
175 and Freschauf, 1973; Schoof and Clarke, 2001) may lead to undulations on the ice stream bed.
176 These spiral flows were proposed to excavate longitudinal grooves and transport the eroded
177 sediments transversely upwards, creating ridges at their sides (Schoof and Clarke, 2001). This
178 hypothesis was initially developed to explain the presence of much smaller flutes and was
179 supported by the observation of 'herring-bone' sediment distribution patterns in mega-flutings,
180 suggesting transverse transport patterns towards ridge crests (Rose, 1987). This theory is similar
181 to the groove-ploughing and meltwater flood theories in the sense that they all assume an
182 erosional-depositional origin of MSGLs (Clark et al., 2003; Shaw et al., 2008).
183

184 1.3. A subglacial bedform continuum

185 The hypothesis of a subglacial bedform continuum invokes morphological relationships
186 between dimensions of different subglacial bedform populations (transverse ribs and ridges,
187 and elongated lineations), which often display a gradual transition downstream (Aario, 1977a,
188 b; Rose, 1987; Clark, 1993; Ely et al., 2016). The continuum is thought to be dependent on ice
189 flow velocity, with longer bedforms being formed through a higher velocity of ice flow (Aario,
190 1977b; Stokes et al., 2013). Although hypothesized for some time and based on only limited
191 observational data (e.g. Aario, 1977a, b; ; Rose, 1987), recent work by Ely et al. (2016) analysed
192 > 96,000 bedforms to clearly demonstrate a link between the morphology of ribbed moraines,
193 drumlins and MSGLs. Thus, a body of evidence has emerged which suggests that MSGLs are
194 at one end of a spectrum of subglacial bedforms that includes ribs, circular bedforms, drumlins
195 and MSGLs (Ely et al., 2016), with the primary control being ice velocity (Barchyn et al., 2016).
196 However, very little work has considered the transitional zone between MSGLs and other
197 features at ice stream grounding lines.
198
199 2. Study area and dataset
200 2.1. Study area
201 The study area is located in the central part of Bjørnøyrenna (Bear Island Trough), SW
202 Barents Sea (Fig.1). During the Last Glacial Maximum (~21 ka BP in this region), the area was
203 occupied by the largest ice stream of the Barents Sea Ice Sheet (BSIS) – the Bjørnøyrenna
204 Palaeo-Ice Stream (Andreassen et al., 2007; Andreassen and Winsborrow, 2009; Winsborrow
205 et al., 2010; Patton et al., 2016; Piasecka et al., 2016). The water depth in the Barents Sea varies
206 from <100 m in the shallow banks to >500 m in the deepest troughs (Jakobsson et al., 2012b).
207 The bathymetry of Bjørnøyrenna ranges from 120 m to ~500 m. The topography of the trough
208 is characterized by a slope deepening downstream with a depth difference of about 30 m
209 between the shallowest and deepest point of the study area and a topographic step further
210 upstream, towards the NE (Fig. 1). Laterally, the trough is bordered by shallow banks (<200 m)

211 in the northern part which potentially created a strong convergence zone for the former ice
212 stream (Fig.1). Farther downstream, the trough curves towards the SW and widens significantly
213 (Fig.1).
214
215 2.2. Dataset
216 This study is based on a modern seafloor reconstructed by mapping the seismic seafloor
217 reflection from a 13,000 km^2 3D seismic dataset located in central Bjørnøyrenna (Fig. 1). The
218 data were provided by Statoil ASA and have vertical and horizontal resolution of 7.4 m,
219 assuming velocity of 1480 m/s for water and dominant frequency 50 Hz for the seismic wave.
220 The data quality is high. A faint NNE-SSW oriented acquisition footprint can be noticed on the
221 reconstructed surface, but this is easily distinguishable and does not hinder interpretation. The
222 seismic interpretation was carried out in Schlumberger Petrel 2014 software. For visualization,
223 the interpreted surface was imported into Fledermaus DMagic v.7 and gridded to a cell size of
224 10 m. This surface was used by Piasecka et al. (2016) to reconstruct a detailed pattern of Late
225 Weichselian flow-switching of the Bjørnøyrenna Palaeo-Ice Stream, largely based on the
226 mapping of ~900 ridge-groove features, interpreted to be MSGLs, forming five distinct flow-
227 sets. The five flow-sets, all identified on the seafloor, cross-cut and overprint each other. All
228 five flow-sets are suggested by Piasecka et al. (2016) to have formed during the mid-phase of
229 the last deglaciation of the Barents Sea Ice Sheet. In this paper, we use ‘’flow-set 8’’ of the five
230 MSGL assemblages, to elucidate the processes of MSGLs formation. This is one of the
231 youngest and is superimposed on other flow-sets (Piasecka et al., 2016). Unique to the mapped
232 flow-sets, the linear MSGL grooves of flow-set 8 transition into curvilinear grooves. Given that
233 this is a fundamental prediction of the groove-ploughing hypothesis (Clark et al., 2003), a key
234 focus of our investigation was to test this MSGL formation mechanism by characterizing
235 variations in MSGL groove amplitude and width.

3. Methods

3.1. Groove depth (amplitude)

Relative depths (amplitudes) of the lineations were extracted by mapping the highest points on the crests and the deepest points of the grooves along each ridge-groove landform in ArcMap v. 10.3 and then calculating the amplitude from absolute depth values (Fig. 2). The points of measurements were initially distributed every 5 km along the grooves. However, due to the post-glacial modification of parts of the surface, such as ploughing and glacimarine deposition (see e.g. Fig. 2), and the overprinting pattern other generations of MSGLs, some of the points located in these modified areas were shifted to obtain representative depth values. The depth values of each groove were plotted along profiles, where the y-axis represents the grooves depths and the x-axis is the distance downstream.

3.2. Groove width

The widths of the grooves were measured using visualization software Fledermaus v. 7, across eight transects for each groove, numbered 1-8 from upstream to downstream, respectively. Due to the lack of an obvious break in slope or 'shoulder' to the grooves, their width was measured as the distance between the highest points (crests) of two associated ridges (Fig. 3c). However, some of the ridges associated with the grooves were eroded or overlain by younger generations of MSGLs and ploughmarks, and their profiles sometimes have several cavities at the crests. This required a determination as to whether the cavity belongs to the groove (and for example was formed by a multi-keel iceberg) or was overprinted by ploughmarks or MSGLs at a later stage (see example in Fig. 2a). This was done based on the orientation of overprinting grooves in 3D view (Fledermaus v. 7) and any cross-cutting grooves were excluded from the measurement. Due to the overprinting patterns, some of the

measurement points were slightly shifted to avoid areas overprinted by other generations of MSGLs, younger ploughmarks, in addition to areas with hemipelagic sediment infills in the grooves. Therefore, the cross-flow profiles for width measurement were not drawn as a straight line.

4. Results

4.1. Linear-curvilinear ridge-groove features

The seafloor relief surface presented in Figure 3 reveals imprints of overprinting and cross-cutting MSGLs assemblages and numerous ploughmarks (Piasecka et al., 2016). Within a large flow set of deglacial MSGLs – ''flow-set 8'', described in Piasecka et al. (2016), we identified numerous features that exhibit both a linear and curvilinear nature. The flow-set has been chosen due to the best preservation of features among all flow-sets, as it is one of the youngest. There seem to be more MSGLs that exhibit transition between curvilinear and linear grooves, but most of them have been overprinted by younger ploughmarks and the continuity is, in these cases, not observable. The continuous features are described and interpreted in the following sections.

a) Description of ridge-groove features

The ridge-groove features (Fig. 4 and 5) are characterized by a linear-curvilinear continuity. They occur on the central Bjørnøyrenna seafloor and their linear orientation is thought to reflect the predominant ice flow direction of the former Bjørnøyrenna Ice Stream (Marfurt, 1998; Andreassen et al., 2008; Andreassen et al., 2014; Bjarnadóttir et al., 2014; Piasecka et al., 2016), curving along the trough towards the SW (Fig. 3). They are characterized by a linear shape along the major part of the groove and display a prominent directional shift further downstream, where they transition into curvilinear grooves (Fig. 5 a-c). Termination of

linear grooves coincides with a thin, but wide, elongated sediment accumulation, up to 10 m in relief, extending across the trough. The pattern of the grooves is, in some areas, distorted by post-glacial modification, such as sediments infilling the grooves or by chaotic patterns of overprinting ploughmarks (see Fig. 2 a). The maximum length of the linear part of the grooves is ~45 km, while the minimum length is 30 km. The maximum length of the grooves (including the curvilinear part of the groove) is ~65 km and the minimum is 41 km. Transition points from linear to curvilinear grooves were identified from directional shifts of the grooves and a noticeable change in groove depth. This occurs at an absolute water depth of about 450-460 m below sea level (bsl), except for two grooves in the southernmost part of the seafloor which are located at a higher elevation (Fig. 5c). Here the transition occurs at present water depths of 443-445 m. Some of the linear parts of the grooves terminate with an overdeepening oriented along the groove axis (Fig. 6, 8) and then the grooves get shallower, once they transition into curvilinear features. Ploughmarks initiate in the outer part of the ice marginal deposit and continue downstream. Some of them can be observed in the deeper part of the trough, away from the grounding line, where they terminate.

b) Interpretation

Based on the length, width and elongation ratio of the grooves we interpret the linear features to be mega-scale glacial lineations (MSGLs), formed through the fast flow of Bjørnøyrenna Palaeo-Ice Stream. According to a recent reconstruction of flow-switching in Bjørnøyrenna (Piasecka et al., 2016), the MSGLs assemblage was formed during one of the ice stream re-advances around 15-16 ka BP, but during overall deglaciation. We interpret the transition line in Figures 5 a-c as the former grounding line around that time and the transverse sediment accumulations as ice marginal deposits. Extent of the inferred grounding line is

delimited by a bathymetric change that shows a topographic deepening of about 10-15 m in the westernmost part of the seafloor.

The MSGLs appear to terminate with keel related overdeepenings (Fig. 6), marking the initiation of each ploughmark and simultaneously indicating reach of the grounded ice. Curvilinear grooves are interpreted as iceberg ploughmarks, similarly to a previous work on this MSGLs assemblage (Piasecka et al., 2016). As such, this is, to our knowledge, the first dataset to clearly demonstrate continuity between the grooves of MSGLs and iceberg ploughmarks (Fig. 5 a-c). Some of the iceberg keels (for example 7, 8, 9, 11, 12 and 13) seem to have continued with an orientation similar to each other (Fig.7). However, others shows much more deviation and we conclude they may have been affected by oceanic currents in front of the ice margin, whereas the others were likely trapped in a dense melange of icebergs. The undulating shape of the inferred grounding line across flow reflects the configuration of the grounded ice margin and the influence of local topography (Fig. 7a).

4.2. Groove depth (amplitude)

a) Description

General trend-lines for all 13 MSGLs show continuous shallowing of the linear grooves downstream (Fig. 8). Slope gradients of the grooves are negative (implicating shallowing) and range from 26% to 3% (14.6° to 1.7°) (Fig. 8). Generally, the depths (amplitudes) of the ridge-groove features fit the definition of MSGLs from numerous settings (Spagnolo et al., 2014). Their relative depths measured between the crest of an MSGL ridge and the deepest point of the associated groove (Fig. 2 and 7) along each groove are plotted in Figure 8. Maximum amplitude values of the measured grooves is 11 m in the upstream part of the ice stream bed (groove number 11), while the minimum is less than 3 m (groove number 3). In the upstream part of the seafloor, the curves show a downstream-decreasing tendency in amplitudes until

335 they reach the point of transition into a ploughmark (Fig. 7, white dashed line). In several cases,
336 the depth profiles show two amplitude peaks (abrupt depth increase) upstream and downstream
337 (grooves 1, 2 and 7). However, in most cases the upstream peak does not occur or is minimal
338 (Fig. 8). Most interestingly, the plots show a prominent deepening in the zone where linear
339 grooves transition into curvilinear grooves. Further downstream, the curvilinear grooves
340 (ploughmarks) depth decreases again until they terminate.
341
342 *b) Interpretation*
343 The landform assemblage of linear-curved grooves is interpreted as mostly erosional, with
344 associated ridges being a by-product of ploughing. The continuity from linear to curvilinear
345 grooves is consistent with erosion by keels at the base of the grounded ice stream which evolve
346 into iceberg keels beyond the grounding line. In the Barents Sea, the observed trough-to-crest
347 amplitude of MSGLs varies between 5 to 10 m (Spagnolo et al., 2014). The relatively minor,
348 yet consistent, decrease in amplitude of the MSGLs assemblage downstream could be explained
349 by melting of the basal ice keels in the ice flow direction (see Discussion).
350
351 4.3. Groove width
352 *a) Description*
353 In contrast to the depth values, width of the grooves exhibit a prominent increase
354 downstream (Fig. 9). The percentage width increase ranges from 5% (117 to 123 m for groove
355 number 13) up to almost 390% (39 to 189 m for groove number 10), see Figure 9b. The widths
356 of MSGLs in the upstream (1) profile vary from 39 m to 131 m. In the middle profile (5), the
357 widths are higher and range from 83 to almost 154 m. In several cases, they are more than twice
358 the upstream width value (groove number 7, 10, 11, 12). In the case of grooves 4 and 13,

however, the value is lower in the main trunk than it is upstream, but increases again in the downstream part.

b) Interpretation

Our results show a general increase in groove width downstream. However, each profile is characterized by a high variability of MSGLs widths, with a broad range of values. MSGLs widen in the ice flow direction, but their width change is most prominent in the downstream part, which would likely represent divergent flow of the ice stream and transition of grooves into ploughmarks (Fig. 5 a-c, Fig. 6). The groove-ploughing formation of MSGLs assumes groove widths to remain constant or decrease downstream (Clark et al., 2003).

5. Discussion

5.1. Testing groove-ploughing predictions

In this section, we discuss the plausibility of a groove-ploughing origin (cf. Clark et al., 2003) for the MSGL-ploughmarks assemblage in central Bjørnøyrenna. A key observation is the clear connection/continuity between MSGLs and ploughmarks. This forms the basis for our groove-ploughing interpretation for Bjørnøyrenna MSGLs because it implies that the same iceberg keel was responsible for creating the connecting groove (MSGL) upstream.

According to predictions of the groove-ploughing theory, MSGLs should occur downstream from where the roughness elements (keels) at the ice stream base are produced (Clark et al., 2003). Typically, roughness in Bjørnøyrenna increases in higher elevations upstream and decreases in deeper basins (e.g. central Bjørnøyrenna) (Gudlaugsson et al., 2013). High bed roughness values have been reported in Bjørnøyrenna upstream from the study area and are likely associated with Triassic subcropping bedrock, which forms a prominent topographic step (Gudlaugsson et al., 2013; Henriksen et al., 2011). Immediately upstream of

384 the studied MSGLs outcropping bedrock ridges, oriented transverse to former ice flow, have
385 been mapped (Bjarnadóttir et al., 2014). Such bedrock undulations may have shaped the ice
386 base, with the resulting basal keels propagating with ice movement downstream into soft-
387 sediments areas (Clark et al., 2003). Downstream, roughness largely decreases towards deeper
388 areas dominated by unconsolidated sediments, which coincide with the initiation of the MSGLs
389 (Gudlaugsson et al., 2013). The area where the mapped MSGLs initiate is dominated by
390 unconsolidated sediments with relatively low roughness.

391 Another factor that was likely important in contributing to the formation of the keels at the
392 ice stream base is the strong convergence zone of Bjørnøyrenna, upstream of the studied
393 MSGLs (Fig. 1). Based on the interpretation of Piasecka et al. (2016), the MSGLs assemblage
394 studied herein is suggested to have formed during deglaciation between 15-16 ka BP. At this
395 time, the ice stream flow trajectory in the study area was entirely constrained within the
396 Bjørnøyrenna trough (Piasecka et al., 2016). Thus, strong lateral compression exerted on the
397 converging ice as it moved through this narrow zone could have created longitudinal structures
398 through shear strain and longitudinal foliation within the ice mass (Clark et al., 2003; Glasser
399 et al., 2015), which further propagated downstream with the ice stream movement. Similar
400 structures, called 'flow stripes', often occur on ice stream surfaces and are created through
401 three-dimensional folding of the ice (Glasser et al., 2015), but may also be a surface expression
402 of bedrock undulations at the ice stream bed (Gudmundsson et al., 1998).

403 A downstream depth decrease of the linear grooves is consistent with groove-ploughing
404 predictions, and is likely an indication of gradual, frictional-related heating and melting of the
405 keels. The presence of ridges at the sides of the grooves suggests they could have formed
406 through squeezing of sediments, eroded from the grooves, away and upwards from the
407 ploughing protuberances and filling in the convex spaces in basal ice, analogous to raking of
408 soil (Clark et al., 2003). Deeper basins of central Bjørnøyrenna are dominated by a layer of

409 unlithified and water-saturated sediments of low roughness (Solheim and Kristoffersen, 1984;
410 Solheim et al., 1990), which are ~60 m thick in the study area. These sediments are mostly of
411 subglacial-glacimarine origin, but are covered by a thin layer of hemipelagic sediments
412 (Solheim and Kristoffersen, 1984). Gradients of the groove depth trend lines (from 26% to 3%)
413 (Fig. 8), suggest a maintenance of ice keels over considerable distances, which could be an
414 indicator of high ice flow velocities and/or the presence of low yield strength, easily deformable
415 sediments at the bed (Clark et al., 2003; Gudlaugsson, 2013). Both are consistent with ice
416 streaming.

417 The width of the curvilinear furrows show a downstream increase (widening), which is a
418 key prediction of the 'groove-ploughing' theory because 'sharper' keels should melt out and
419 become broader and flatter. Indeed, widening of the linear grooves downstream can result from
420 a combination of extensional ice flow in the divergence zone and gradual melting of the keels
421 through ploughing of the sediments (frictional heating) (Benn and Evans, 2010). Consistent
422 with groove-ploughing predictions, the spacing between the MSGLs slightly increases
423 downstream, most likely due to ice stream flow divergence. Although the spacing increase is
424 not large, it becomes more prominent with the initiation of curvilinear grooves at the inferred
425 grounding line. Transition into ploughmarks points to activity of free icebergs, detached from
426 the grounded ice margin and scouring at present water depths of ~450 m (Fig. 7). At that time,
427 the relative sea level was 110-115 m less than it is today, while ice thickness was at least twice
428 the water depth (Andreassen et al., 2017; Patton et al., 2016). The continuity of MSGLs and
429 ploughmarks is consistent with the groove-ploughing theory, predicting a sharp change in shape
430 of the grooves, as well as directional shifts of grooves, at the inferred grounding line.
431

432 5.2. MSGL-ploughmark transition at the grounding line

433 The abrupt shift in groove orientation and the deepening of the groove at the end of each
434 MSGL (Fig. 6) likely marks the grounding line and the transition from a MSGL groove to an
435 iceberg ploughmark (Fig. 5 a-c). The increase in groove depth at the end of each MSGL, where
436 they transition into ploughmarks, is somewhat enigmatic, but may have resulted from the
437 impact of an iceberg being abruptly detached from the grounded ice front, whereupon it loses
438 its lateral buttressing and temporarily sinks and grounds on the seafloor (King et al., 2016).
439 Although the bathymetry seems deep in the area (present depth 450 m bsl), the thickness of the
440 ice margin was enough for detached icebergs to ground (Andreassen et al., 2017; Patton et al.,
441 2015; 2016). Such deep-water iceberg ploughing is commonly observed on the Arctic
442 continental shelf down to at least 500 m water depth, but there are examples of iceberg
443 ploughing in depths reaching 850 m (Vogt et al., 1994).
444 Palaeo-climate reconstructions indicate that as the ice margin entered deeper water, it may
445 have been affected by the influx of Norwegian Atlantic Current (>3°C) during the late glacial
446 around 16 ka BP (Ślubowska-Woldengen et al., 2008), and which may have undercut the ice at
447 its base. The presence of the warm current at the ice front and deepening of the trough
448 downstream along its axis, could have prevented formation of an ice shelf, instead exposing an
449 ice wall (Pollard et al., 2015). After calving, some of the icebergs seemed to follow the slight
450 overdeepening in the westernmost part of the seafloor, perhaps still influenced by the warm
451 Atlantic Current (Ślubowska-Woldengen et al., 2008). These processes at the grounding line
452 are illustrated in Fig. 10, which shows a conceptual model of how the MSGL grooves transition
453 into iceberg ploughmarks. Configuration of the inferred grounding line might have been
454 determined by the distribution of surface and bottom crevasses, as well as the regional
455 topography. There is no data regarding presence of an ice shelf in the study area, however, we
456 may imply a grounded ice stream terminus (as evidenced by the continuity of grooves).
457

458 5.3. Comparison of results with other theories of MSGL formation

459 We consider groove-ploughing to be the primary mechanism in formation of the subset of
460 Bjørnøyrenna MSGLs described in this study, largely because of the strong observational
461 evidence that shows that grooves associated with MSGLs transition into iceberg ploughmarks,
462 the latter being clearly erosional. Given that not all MSGLs within the dataset show this
463 bedform continuum, we do not suggest that groove-ploughing is the only mechanism for MSGL
464 formation. However, we clearly document this to be one of the mechanisms by which MSGLs
465 can be formed and now evaluate other possible mechanisms of MSGL formation in light of our
466 observations.

467 The sediment deformation theory (Clark, 1993), is unlikely to be the primary mechanism
468 for the Bjørnøyrenna MSGLs-ploughmarks continuum because the iceberg ploughmarks are
469 clearly erosional, and can be traced upstream into the grooves that lie between MSGLs. Inherent
470 to traditional views of the deforming bed theory (e.g. Boulton and Hindmarsh, 1987), is that
471 sediment deformation occurs around substrate irregularities that seed the glacial lineation (e.g.
472 drumlins or MSGLs). Such substrate irregularities at the stoss end of MSGLs are not obvious
473 in our datasets and, indeed, the start and end of the MSGL ridges either side of the grooves are
474 not always easy to identify (cf. Spagnolo et al., 2014). Moreover, under conditions of a
475 pervasively deforming bed, it might be expected that drumlins should form upstream of the
476 MSGLs in the onset zone of the ice stream (e.g. showing a bedform continuum with an
477 increasing degree of streamlining and elongation down-ice as velocities increase). However, no
478 drumlins have been mapped upstream of the study area in Bjørnøyrenna. There are, however,
479 some observations of 'shoulders' on the flanks of grooves, which may suggest that material is
480 locally ploughed from within the groove and pushed and squeezed up towards ridge crests
481 (Clark et al., 2003). In some senses, this is a form of deformation that is associated with the
482 groove-ploughing process (cf. O'Cofaigh et al., 2013), but we do not consider it a major process

in the formation of the intervening ridges (MSGLs), which we instead view as largely erosional remnants.

The mega flood theory (Shaw et al., 2008) implies the presence of meltwater bedforms (meltwater channels, eskers, tunnel valleys) in association with the assemblage of MSGLs. However, no such forms have been observed upstream of the study area (Bjarnadóttir et al., 2014). Landforms in upper Bjørnøyrenna are mostly associated with fast ice stream flow or ice stream stagnation, with no signs of catastrophic meltwater release (Andreassen et al., 2014; Bjarnadóttir et al., 2014). Two flow-sets of MSGLs overprint our sample assemblage (Piasecka et al., 2016) and we find it unlikely that multiple generations of flow-sets could be preserved if they were formed by catastrophic floods. Therefore, we suggest that the MSGLs in Bjørnøyrenna are formed by a mechanism unrelated to catastrophic meltwater floods.

The rilling instability theory for MSGL formation (Fowler, 2010) has thus far been difficult to test empirically. There is no doubt that meltwater pressure and, hence, porewater pressure in sediments, has had a key effect on the generation of the Bjørnøyrenna flow-sets, and likely facilitated the fast ice flow. Moreover, the rilling instability could explain how grooves are excavated by a combination of ice-keel ploughing and localized meltwater erosion within the groove. It is plausible therefore that when this undulating base comes afloat the keels within grooves also create ploughmarks. However, the theory predicts a regular distribution of MSGLs with 'preferred' dimensions (Fowler, 2010). The dimensions of the MSGLs within the Bjørnøyrenna flow-set are broadly consistent with these predictions, but show a wider range in both width and vertical amplitude and their distribution is not obviously regular and awaits further quantitative analysis.

To summarise, we suggest that MSGLs are likely formed through a combination of several mechanisms, such as groove-ploughing (Clark et al., 2003), sediment deformation along the flanks of the grooves, and perhaps focussed meltwater erosion within the grooves (Fowler,

2010). However because there is such a clear continuity between the erosional iceberg ploughmarks and the grooves upstream that sit between the MSGLS, we suggest that groove-ploughing is the dominant formation mechanism of the landform assemblage.

6. Conclusions

MSGLs are important to understanding ice stream dynamics, but there is little consensus regarding their formation (Stokes et al., 2013; Spagnolo et al., 2016; Stokes, in press). Conclusions of numerous studies from different palaeo-ice stream beds raise the possibility of a complex origin of MSGLs (e.g. King et al., 2009; Ó Cofaigh et al., 2013; Stokes et al., 2013; Spagnolo et al., 2016), often indicating groove-ploughing as a secondary or a localised process contributing to their formation (Stokes et al., 2013; Spagnolo et al., 2014). In this paper, we present observations of MSGLs from the bed of the former Bjørnøyrenna Ice Stream, SW Barents Sea that clearly show that a subset of these landforms exhibit a transition from an assemblage of grooves associated with MSGLs to iceberg ploughmarks. This points to groove-ploughing of ice keels as primary dominant formational process for this subset of MSGLs. The linear part of the grooves is inferred to have formed through groove-ploughing of sediments by ice keels at the ice stream base (cf. Clark et al., 2003). This is supported primarily by the continuity from linear (MSGLs) to curvilinear grooves (ploughmarks) and the downstream-decreasing depth of the grooves and the slight downstream-increase in spacing of the grooves. Ice base undulations could have formed in higher roughness zones in northern Bjørnøyrenna and are likely to have been amplified in the strong convergence zone upstream from the study area. Soft, weak sediments in the deeper parts of central Bjørnøyrenna could sustain fast ice flow and allow propagation of the ice keels farther downstream. In summary, we document clear evidence for MSGLs in central Bjørnøyrenna forming by a groove-ploughing mechanism, evidence that in some settings this is an important subglacial process.

Acknowledgements:

This work is a contribution to “Glaciated North Atlantic Margins” (GLANAM) Initial Training Network funded by the European Community's 7th Framework Programme FP7 2007/2013, Marie-Curie Actions, under Grant Agreement No. 317217. It is also a part of ”CAGE” – “the Centre for Arctic Gas Hydrate, Environment and Climate” , supported by the Research Council of Norway through its Centres of Excellence funding scheme grant No. 223259. The 3D seismic dataset was kindly provided by Statoil ASA and TGS Norway.

Figure captions:

Fig. 1 Overview map of the study area in central Bjørnøyrenna (Bear Island Trough), SW Barents Sea. The black outline indicates the location of the seafloor image presented in Fig. 3. Orange dashed lines show the extent of the trough with the convergence zone in its northern part, diverging downstream (blue dashed line). Orange arrows indicate ice flow direction of the Bjørnøyrenna Palaeo-Ice Stream during deglaciation. The background map is taken from IBCAO v. 3.0 (Jakobsson et al., 2012b). Inset figure shows the extent of the Barents Sea-Fennoscandian Ice Sheet during its Last Glacial Maximum (blue outline) and the black box shows the location of the overview map.

Fig. 2 Illustration of ridge-groove amplitude (depth) measurements. (a) A ridge-groove curvilinear feature. Inset shows the location of the figure on the seafloor map. (b) Red point indicates the crest of the associated ridge (highest point), the blue point is the deepest value within the groove. (c) Profile x-y showing depth difference between the deepest and the shallowest point.

Fig. 3 (a) Shaded relief surface of the seafloor reconstructed from 3D seismic data. Black arrows indicate the orientation of acquisition artifacts. (b) Seafloor showing mapping of the complete MSGLs assemblage, displaying some linear-curvilinear characteristics where MSGLs grooves transition into ploughmarks. (c) Illustration of groove width measurement. The black arrows indicate distance between two MSGL ridge crests

Fig. 4 Map of the Bjørnøyrenna seafloor showing the linear-sinusoidal grooves assemblage used in this study (black lines). Black rectangles mark the location of zoom-ins shown in Figure 5, while white rectangles indicate the location of close-ups of transition points (deeper iceberg 'pits') initiating curvilinear grooves (Fig. 6).

Fig. 5 A magnified view of linear grooves transitioning into curvilinear ploughmarks (for location see Fig. 4). White arrows point to the linear part of the grooves (MSGLs), while the black arrows point to the sinusoidal part (ploughmarks). The orange circles mark the approximate point of transition and the dashed white lines represent the inferred grounding line based on that transition.

Fig. 6 Examples of pits made by ploughing keels (dashed black circles) which mark the transition from linear to curvilinear groove (for location see Fig. 4). Along-groove profiles (orange line) show an abrupt depth change at the transition from linear to curvilinear groove. Blue dashed vertical lines on the profiles mark the point along the groove where the MSGL transitions into a ploughmark.

Fig. 7 Ridge-groove features showing transition from linear to curvilinear shape. The orange dots indicate depth (amplitude) measurement points along each ridge-groove (Fig. 8). The white

582 dashed line indicates the transition points from linear to curvilinear grooves (presumably the
583 former grounding line).
584
585 **Fig. 8** Stacked groove amplitude curves showing the depth-decreasing trend of the studied
586 grooves. Vertical axis represents depths of the grooves (in meters). The horizontal axis indicates
587 subglacial and proglacial part of the grooves, inferred from the directional shift of linear into
588 curvilinear grooves and their sudden depth increase. The dashed vertical line marks the inferred
589 grounding line. Numbers to the left indicate the designation number of a groove and correspond
590 to the numbers of MSGLs in Fig. 7.
591
592 **Fig. 9** (a) Analysis of groove widths. Numbers 1-8 indicate cross-profile locations (transect
593 numbers on x-axis), where (1) is the upstream profile and (8) is the downstream profile (b)
594 Values of all groove widths (in meters) plotted for the eight cross-profiles. Each colour indicates
595 one MSGL, from number 1 to 13.
596
597 **Fig. 10**. (a) Conceptual model of the MSGLs-ploughmark formation through slab calving at a
598 grounded ice cliff. Numbers 1-5 indicate particular stages of ice flow and calving. 1 –
599 Bjørnøyrenna Palaeo-Ice Stream readvance towards the deeper parts of Bjørnøyrenna; 2 – the
600 grounding line shifts towards the deeper basin in central Bjørnøyrenna and crevasses start to
601 form; 3 – extensional strain due to divergent flow and tensile stresses near the terminus resulting
602 from depth differences (Δh) lead to fracture formation; 4 – the fracture eventually connects
603 surface and bottom crevasse, possibly leading to slab calving; 5 – the detached iceberg falls to
604 the deeper water, forming a pit (black circle) through keel impact, and scours the seafloor as it
605 moves downstream, creating a ploughmark (dark green curve). Transition line indicated with
606 red dashed line. (b) A simplified illustration of the Bjørnøyrenna Palaeo-Ice Stream groove-

ploughing (modified from Clark et al., 2003). The dashed lines show grooves created by the ice stream keels during the readvance.

610 **References:**

611 Aario, R., 1977a. Associations of flutings, drumlins, hummocks and transverse ridges.
612 GeoJournal 1, 65-72.

613 Aario, R., 1977b. Classification and terminology of morainic landforms in Finland. Boreas 6,
614 87-100.

615 Andreassen, K., Hubbard, A., Winsborrow, M., Patton, H., Vadakkepuliyambatta, S., Plaza-
616 Faverola, A., Gudlaugsson, E., Serov, P., Deryabin, A., Mattingsdal, R., Mienert, J., Bünz,
617 S., 2017. Massive blow-out craters formed by hydrate-controlled methane expulsion from
618 the Arctic seafloor. Science 356**,** 948-953

619 Andreassen, K., Laberg, J.S., Vorren, T.O., 2008. Seafloor geomorphology of the SW Barents
620 Sea and its glaci-dynamic implications. Geomorphology 97, 157-177.

621 Andreassen, K., Winsborrow, M., 2009. Signature of ice streaming in Bjørnøyrenna, Polar
622 North Atlantic, through the Pleistocene and implications for ice-stream dynamics. Annals of
623 Glaciology 50, 17-26.

624 Andreassen, K., Winsborrow, M.C.M., Bjarnadóttir, L.R., Rüther, D.C., 2014. Ice stream
625 retreat dynamics inferred from an assemblage of landforms in the northern Barents Sea.
626 Quaternary Science Reviews 92, 246-257.

627 Andreassen, K., Ødegaard, C.M., Rafaelsen, B., 2007. Imprints of former ice streams, imaged
628 and interpreted using industry three-dimensional seismic data from the south-western
629 Barents Sea. Geological Society, London, Special Publications 277, 151-169.

630 Bamber, J.L., Vaughan, D.G., Joughin, I., 2000. Widespread Complex Flow in the Interior of
631 the Antarctic Ice Sheet. Science 287, 1248-1250.

632 Barchyn, T.E., Dowling, T.P.F., Stokes, C.R., Hugenholtz, C.H., 2016. Subglacial bed form
633 morphology controlled by ice speed and sediment thickness. Geophysical Research Letters
634 43, 7572-7580.

635 Bell, R.E., Blankenship, D.D., Finn, C.A., Morse, D.L., Scambos, T.A., Brozena, J.M., Hodge,
636 S.M., 1998. Influence of subglacial geology on the onset of a West Antarctic ice stream from
637 aerogeophysical observations. Nature 394, 58-62.
638 Benn, D.I., Evans, D.J.A., 2010. Glaciers and Glaciation, Second Edition ed. Routlege, New
639 York.
640 Bennett, M.R., 2003. Ice streams as the arteries of an ice sheet: their mechanics, stability and
641 significance. Earth-Science Reviews 61, 309-339.
642 Bentley, C.R., Giovinetto, M.B., 1991. Mass balance of Antarctica and sea level change., in:
643 Weller, G., Wilson, C.L., Sevberin, B.A.B. (Eds.), International Conference on the Role of
644 the Polar Regions in Global Change: Proceedings of a Conference Held June 11–15, 1990
645 at the University of Alaska Fairbanks. Geophysical Institute/Centre for Global Change and
646 Arctic Sys- tems Research, Fairbanks, pp. 481-488.
647 Bjarnadóttir, L.R., Winsborrow, M.C.M., Andreassen, K., 2014. Deglaciation of the central
648 Barents Sea. Quaternary Science Reviews 92, 208-226.
649 Boulton, G.S., Hindmarsh, R.C.A., 1987. Sediment deformation beneath glaciers: Rheology
650 and geological consequences. Journal of Geophysical Research 92, 9059.
651 Clark, C.D., 1993. Mega-scale glacial lineations and cross-cutting ice-flow landforms. Earth
652 Surface Processes and Landforms 18, 1-29.
653 Clark, C.D., 1999. Glaciodynamic context of subglacial bedform generation and preservation.
654 Annals of Glaciology 28, 23-32.
655 Clark, C.D., Tulaczyk, S., Stokes, C.R., Canals, M., 2003. A groove-ploughing theory for the
656 production of mega-scale glacial lineations, and implications for ice-stream mechanics.
657 Journal of Glaciology 49, 240-256.
658 Clarke, G.K.C., Leverington, D.W., Telle, J.T., Dyke, A.S., Marshall, S.J., 2005. Fresh
659 arguments against the Shaw megaflood hypothesis. A reply to comments by David Sharpe

660 on ‘Palaeohydraulics of the last outburst flood from glacial-Lake Agassiz and the 8200 BP
661 cold event’. Quaternary Science Reviews 24, 1533–1541.
662 Dowdeswell, J.A., Hogan, K.A., Evans, J., Noormets, R., Cofaigh, C.O., Ottesen, D., 2010. Past
663 ice-sheet flow east of Svalbard inferred from streamlined subglacial landforms. Geology 38,
664 163-166.
665 Ely, J.C., Clark, C.D., Spagnolo, M., Stokes, C.R., Greenwood, S.L., Hughes, A.L.C., Dunlop,
666 P., Hess, D., 2016. Do subglacial bedforms comprise a size and shape continuum?
667 Geomorphology 257, 108-119.
668 Evans, D.J.A., Twigg, D.R., 2002. The active temperate glacial landsystem: a model based on
669 Breiðamerkurjökull and Fjallsjökull, Iceland. Quaternary Science Reviews 21, 2143-2177.
670 Fowler, A.C., 2010. The formation of subglacial streams and mega-scale glacial lineations.
671 Proceedings of the Royal Society A: Mathematical, Physical and Engineering Sciences 466,
672 3181-3201.
673 Glasser, N.F., Jennings, S.J.A., Hambrey, M.J., Hubbard, B., 2015. Origin and dynamic
674 significance of longitudinal structures ("flow stripes") in the Antarctic Ice Sheet. Earth Surf.
675 Dynam. 3, 239-249.
676 Graham, A.G.C., Larter, R.D., Gohl, K., Hillenbrand, C.-D., Smith, J.A., Kuhn, G., 2009.
677 Bedform signature of a West Antarctic palaeo-ice stream reveals a multi-temporal record of
678 flow and substrate control. Quaternary Science Reviews 28, 2774-2793.
679 Gudlaugsson, E., Humbert, A., Winsborrow, M., Andreassen, K., 2013. Subglacial roughness
680 of the former Barents Sea ice sheet. Journal of Geophysical Research: Earth Surface 118,
681 2546-2556.
682 Gudmundsson, G.H., Raymond, C.F., Bindschadler, R., 1998. The origin and longevity of flow
683 stripes on Antarctic ice streams. Annals of Glaciology 27, 145-152.

684 Henriksen, E., Bjørnseth, H., Hals, T., Heide, T., Kiryukhina, T., Kløvjan, O., Larssen, G.,
685 Ryseth, A., Rønning, K., and Sollid, K., 2011. Uplift and erosion of the greater Barents Sea:
686 impact on prospectivity and petroleum systems: Geological Society, London, Memoirs, v.
687 35, no. 1, p. 271- 281.
688 Hogan, K.A., Dowdeswell, J.A., Noormets, R., Evans, J., Ó Cofaigh, C., Jakobsson, M., 2010.
689 Submarine landforms and ice-sheet flow in the Kvitøya Trough, northwestern Barents Sea.
690 Quaternary Science Reviews 29, 3545-3562.
691 Holt, J.W., Blankenship, D.D., Morse, D.L., Young, D.A., Peters, M.E., Kempf, S.D., Richter,
692 T.G., Vaughan, D.G., Corr, H.F.J., 2006. New boundary conditions for the West Antarctic
693 Ice Sheet: Subglacial topography of the Thwaites and Smith glacier catchments. Geophysical
694 Research Letters 33.
695 Jakobsson, M., Anderson, J.B., Nitsche, F.O., Gyllencreutz, R., Kirshner, A.E., Kirchner, N.,
696 O'Regan, M., Mohammad, R., Eriksson, B., 2012a. Ice sheet retreat dynamics inferred from
697 glacial morphology of the central Pine Island Bay Trough, West Antarctica. Quaternary
698 Science Reviews 38, 1-10.
699 Jakobsson, M., Mayer, L., Coakley, B., Dowdeswell, J.A., Forbes, S., Fridman, B., Hodnesdal,
700 H., Noormets, R., Pedersen, R., Rebesco, M., Schenke, H.W., Zarayskaya, Y., Accettella,
701 D., Armstrong, A., Anderson, R.M., Bienhoff, P., Camerlenghi, A., Church, I., Edwards, M.,
702 Gardner, J.V., Hall, J.K., Hell, B., Hestvik, O.B., Kristoffersen, Y., Marcussen, C.,
703 Mohammad, R., Mosher, D., Nghiem, S.V., Pedrosa, M.T., Travaglini, P.G., Weatherall, P.,
704 2012b. The International Bathymetric Chart of the Arctic Ocean (IBCAO) Version 3.0.
705 Geophysical Research Letters 39.
706 King, E.C., Hindmarsh, R.C.A., Stokes, C.R., 2009. Formation of mega-scale glacial lineations
707 observed beneath a West Antarctic ice stream. Nature Geoscience 2, 585-588.

King, E.L., Rise, L., Bellec, V.K., 2016. Crescentic submarine hills and holes produced by iceberg calving and rotation. Atlas of Submarine glacial landforms, p. 267-268.

Livingstone, S.J., Ó Cofaigh, C., Stokes, C.R., Hillenbrand, C.-D., Vieli, A., Jamieson, S.S.R., 2012. Antarctic palaeo-ice streams. Earth-Science Reviews 111, 90-128.

Marfurt, K.J., 1998. Suppression of the acquisition footprint for seismic attribute mapping. Geophysics 63, 1024-1035.

Margold, M., Stokes, C.R., Clark, C.D., 2015. Ice streams in the Laurentide Ice Sheet: Identification, characteristics and comparison to modern ice sheets. Earth-Science Reviews 143, 117-146.

Nitsche, F.O., Gohl, K., Larter, R.D., Hillenbrand, C.D., Kuhn, G., Smith, J.A., Jacobs, S., Anderson, J.B., Jakobsson, M., 2013. Paleo ice flow and subglacial meltwater dynamics in Pine Island Bay, West Antarctica. The Cryosphere 7, 249-262.

Ó Cofaigh, C., Dowdeswell, J.A., Allen, C.S., Hiemstra, J.F., Pudsey, C.J., Evans, J., J.A. Evans, D., 2005. Flow dynamics and till genesis associated with a marine-based Antarctic palaeo-ice stream. Quaternary Science Reviews 24, 709-740.

Ó Cofaigh, C., Dowdeswell, J.A., King, E.C., Anderson, J.B., Clark, C.D., Evans, D.J.A., Evans, J., Hindmarsh, R.C.A., Larter, R.D., Stokes, C.R., 2010. Comment on Shaw J., Pugin, A. and Young, R. (2008): "A meltwater origin for Antarctic shelf bedforms with special attention to megalineations", Geomorphology 102, 364–375. Geomorphology 117, 195-198.

Ó Cofaigh, C., Pudsey, C.J., Dowdeswell, J.A., Morris, P., 2002. Evolution of subglacial bedforms along a paleo-ice stream, Antarctic Peninsula continental shelf. Geophysical Research Letters 29, 41-41-41-44.

Ó Cofaigh, C., Stokes, C.R., Lian, O.B., Clark, C.D., Tulacyzk, S., 2013. Formation of mega-scale glacial lineations on the Dubawnt Lake Ice Stream bed: 2. Sedimentology and stratigraphy. Quaternary Science Reviews 77, 210-227.

733 Ottesen, D., Dowdeswell, J.A., Rise, L., 2005. Submarine landforms and the reconstruction of
734 fast-flowing ice streams within a large Quaternary ice sheet: The 2500-km-long Norwegian-
735 Svalbard margin (57°–80°N). Geological Society of America Bulletin 117, 1033.
736 Patton, H., Andreassen, K., Bjarnadóttir, L.R., Dowdeswell, J.A., Winsborrow, M., Noormets,
737 R., Polyak, L., Auriac, A., Hubbard, A., 2015. Geophysical constraints on the dynamics and
738 retreat of the Barents Sea ice sheet as a paleobenchmark for models of marine ice sheet
739 deglaciation. Reviews of Geophysics 185-217.
740 Patton, H., Hubbard, A., Andreassen, K., Winsborrow, M., Stroeven, A.P., 2016. The build-up,
741 configuration, and dynamical sensitivity of the Eurasian ice-sheet complex to Late
742 Weichselian climatic and oceanic forcing. Quaternary Science Reviews 153, 97-121.
743 Piasecka, E.D., Winsborrow, M.C.M., Andreassen, K., Stokes, C.R., 2016. Reconstructing the
744 retreat dynamics of the Bjørnøyrenna Ice Stream based on new 3D seismic data from the
745 central Barents Sea. Quaternary Science Reviews 151, 212-227.
746 Pollard, D., DeConto, R., Alley, R., 2015. Potential Antarctic Ice Sheet retreat driven by
747 hydrofracturing and ice cliff failure. Earth and Planetary Science Letters 412, 112-121.
748 Robel, A. A., Tziperman, E., 2016. The role of ice stream dynamics in deglaciation. Journal of
749 Geophysical Research: Earth Surface 121, 1540-1554.
750 Rose, J., 1987. Drumlins as part of a glacier bedform continuum. Drumlin symposium.
751 Manchester, 1985, 103-116.
752 Schoof, C., Clarke, G.K.C., 2001. A model for spiral flows in basal ice and the formation of
753 subglacial flutes based on Reiner-Rivlin rheology for glacial ice. Journal of Geophysical
754 Research.
755 Shaw. J., 1983. Drumlin formation related to inverted melt-water erosional marks. Journal of
756 Glaciology 29, 185-214.

757 Shaw, J., Freschauf, R.C., 1973. A kinematic discussion of the formation of glacial flutings.
758 Canadian Geographer / Le Géographe canadien 17, 19-35.
759 Shaw, J., Pugin, A., Young, R.R., 2008. A meltwater origin for Antarctic shelf bedforms with
760 special attention to megalineations. Geomorphology 102, 364-375.
761 Shaw, J., and Sharpe, D.R., 1987. Drumlin formation by subglacial meltwater erosion.
762 Canadian Journal of Earth Sciences 24, 2316-2322.
763 Slubowska-Woldengen, M. A., Rasmussen, T., Koc, N., Klitgaard-Kristensen, D., Nilsen, F.,
764 Solheim, A., 2007. Advection of Atlantic Water to the western and northern Svalbard shelf
765 since 17,500 cal yr BP. Quaternary Science Reviews 26, 463- 478.
766 Smith, A.M., Murray, T., 2009. Bedform topography and basal conditions beneath a fast-
767 flowing West Antarctic ice stream. Quaternary Science Reviews 28, 584-596.
768 Smith, A.M., Murray, T., Nicholls, K.W., Makinson, K., Aðalgeirsdóttir, G., Behar, A.E.,
769 Vaughan D.G., 2007. Rapid erosion, drumlin formation, and changing hydrology beneath an
770 Antarctic ice stream. Geology 35, 127–130.
771 Solheim, A., Kristoffersen, Y., 1984. Physical environment Western Barents Sea, 1: 1,500,000;
772 sediments above the upper regional unconformity: thickness, seismic stratigraphy and
773 outline of the glacial history. Norsk Polarinstitutt Skrifter 179B, 3-26.
774 Solheim, A., Russwurm, L., Elverhøi, A., Berg, M.N. 1990. Glacial geomorphic features in the
775 northern Barents Sea: direct evidence for grounded ice and implications for the pattern of
776 deglaciation and late glacial sedimentation. Glacimarine Enviroments: Processes and
777 Sediments. J. A. Dowdeswell and J. D. Scourse. London, The Geological Society 53, 253-
778 268.
779 Spagnolo, M., Clark, C.D., Ely, J.C., Stokes, C.R., Anderson, J.B., Andreassen, K., Graham,
780 A.G.C., King, E.C., 2014. Size, shape and spatial arrangement of mega-scale glacial

781 lineations from a large and diverse dataset. Earth Surface Processes and Landforms, 1432-
782 1448.
783 Spagnolo, M., Phillips, E., Piotrowski, J.A., Rea, B.R., Clark, C.D., Stokes, C.R., Carr, S.J.,
784 Ely, J.C., Ribolini, A., Wysota, W., Szuman, I., 2016. Ice stream motion facilitated by a
785 shallow-deforming and accreting bed. Nature Communications 7.
786 Stokes, C. R., (in press). Geomorphology under ice streams: Moving from form to process.
787 Earth Surface Processes and Landforms.
788 Stokes, C.R., Clark, C.D., 2001. Palaeo-ice streams. Quaternary Science Reviews 20, 1437-
789 1457.
790 Stokes, C.R., Clark, C.D., 2003. Giant glacial grooves detected on Landsat ETM+ satellite
791 imagery. International Journal of Remote Sensing 24, 905-910.
792 Stokes, C. R., Clark, C.D., Lian, O.B., Tulaczyk, S., 2007. Ice stream sticky spots: A review of
793 their identification and influence beneath contemporary and palaeo-ice streams. Earth-
794 Science Reviews 81, 217-249.
795 Stokes, C. R., Margold, M., Clark, C. D., Tarasov, L., 2016. Ice stream activity scaled to ice
796 sheet volume during Laurentide Ice Sheet deglaciation. Nature 530, 322-326.
797 Stokes, C.R., Spagnolo, M., Clark, C.D., Ó Cofaigh, C., Lian, O.B., Dunstone, R.B., 2013.
798 Formation of mega-scale glacial lineations on the Dubawnt Lake Ice Stream bed: 1. size,
799 shape and spacing from a large remote sensing dataset. Quaternary Science Reviews 77, 190-
800 209.
801 Tulaczyk, S., Kamb, W.B., Engelbardt, H.F., 2000. Basal mechanics of Ice Stream B, West
802 Antarctica 2. Undrained plastic bed model. Journal of Geophysical Research-Solid Earth
803 105, 483-494.
804 Tulaczyk, S., Scherer, R.P., Clark, C.D., 2001. A ploughing model for the origin of weaktills
805 beneath ice streams. Quaternary International 86, 59-70.

806 Vogt, P. R., Crane, E., Sundvor, E. 1994. Deep Pleistocene iceberg plowmarks on the Yermak
807 Plateau: Sidescan and 3.5 kHz evidence for thick calving ice fronts and a possible marine
808 ice sheet in the Arctic Ocean. Geology 22, 403-406.
809 Winsborrow, M.C.M., Andreassen, K., Corner, G.D., Laberg, J.S., 2010. Deglaciation of a
810 marine-based ice sheet: Late Weichselian palaeo-ice dynamics and retreat in the southern
811 Barents Sea reconstructed from onshore and offshore glacial geomorphology. Quaternary
812 Science Reviews 29, 424-442.
813 Winsborrow, M., Andreassen, K., Hubbard, A., Plaza-Faverola, A., Gudlaugsson, E., Patton,
814 H., 2016. Regulation of ice stream flow through subglacial formation of gas hydrates. Nature
815 Geoscience 9, 370-374.
816 Winsborrow, M.C.M., Stokes, C.R., Andreassen, K., 2012. Ice-stream flow switching during
817 deglaciation of the southwestern Barents Sea. Geological Society of America Bulletin 124,
818 275-290.

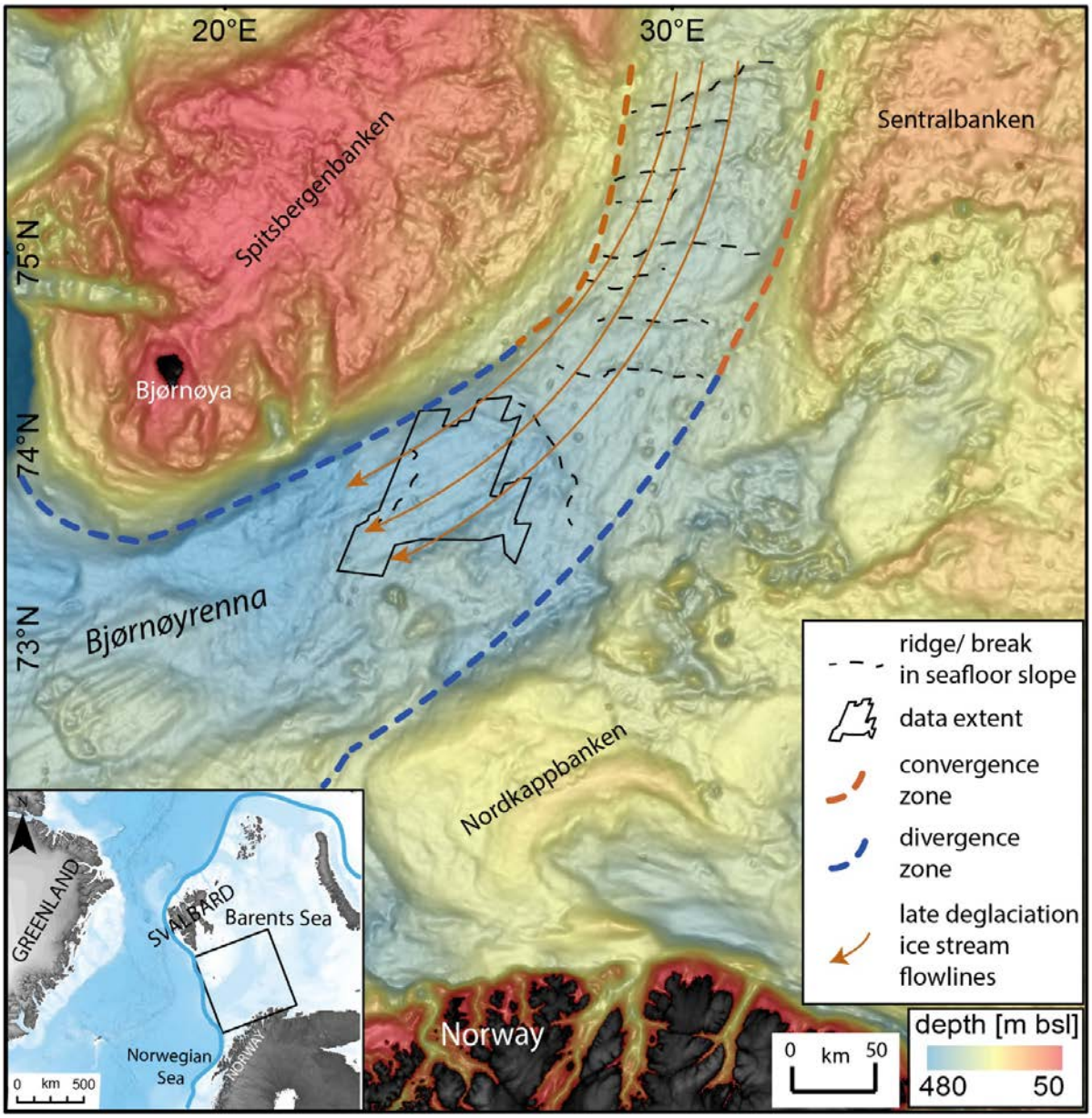
20°E
30°E
75°N
74°N
73°N
Spitsbergenbanken
Sentralbanken
Bjørnøya
Bjørnøyrenna
Nordkappbanken
Norway
ridge/ break in seafloor slope
data extent
convergence zone
divergence zone
late deglaciation ice stream flowlines
depth [m bsl]
480
50
0 km 50
GREENLAND
SVALBARD
Barents Sea
Norwegian Sea
NORWAY
0 km 500

819

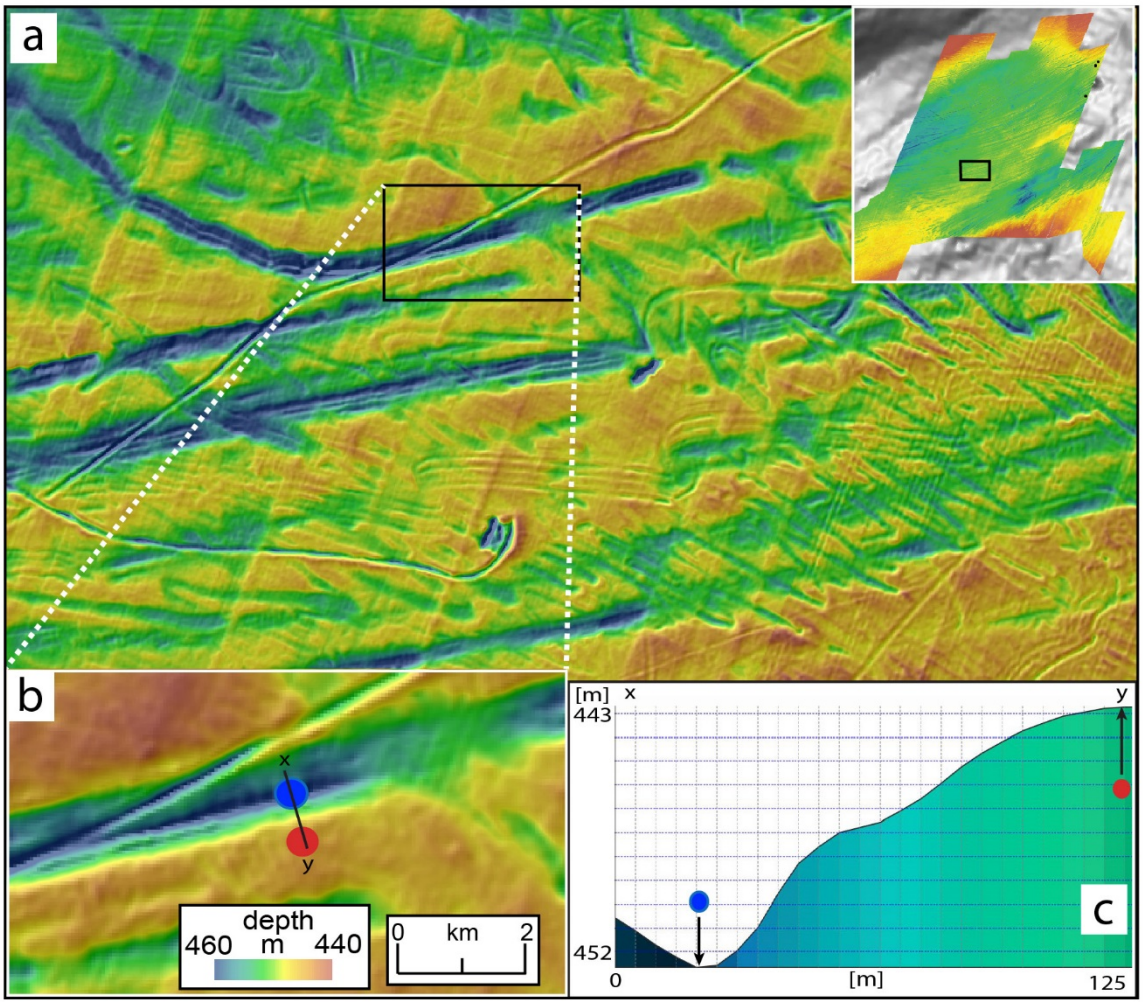

820

a
24°E
74°N
acquisition artifacts
depth
480 m 390
km
0 5 10
b
24°E
74°N
depth
480 m 390
km
0 5 10
x
y
c
groove width
x
y
Depth [m]
-452
-454
-456
NNW
SSE
Distance [km]
0 1 2 3 4 5 6 7 8 9 10

821

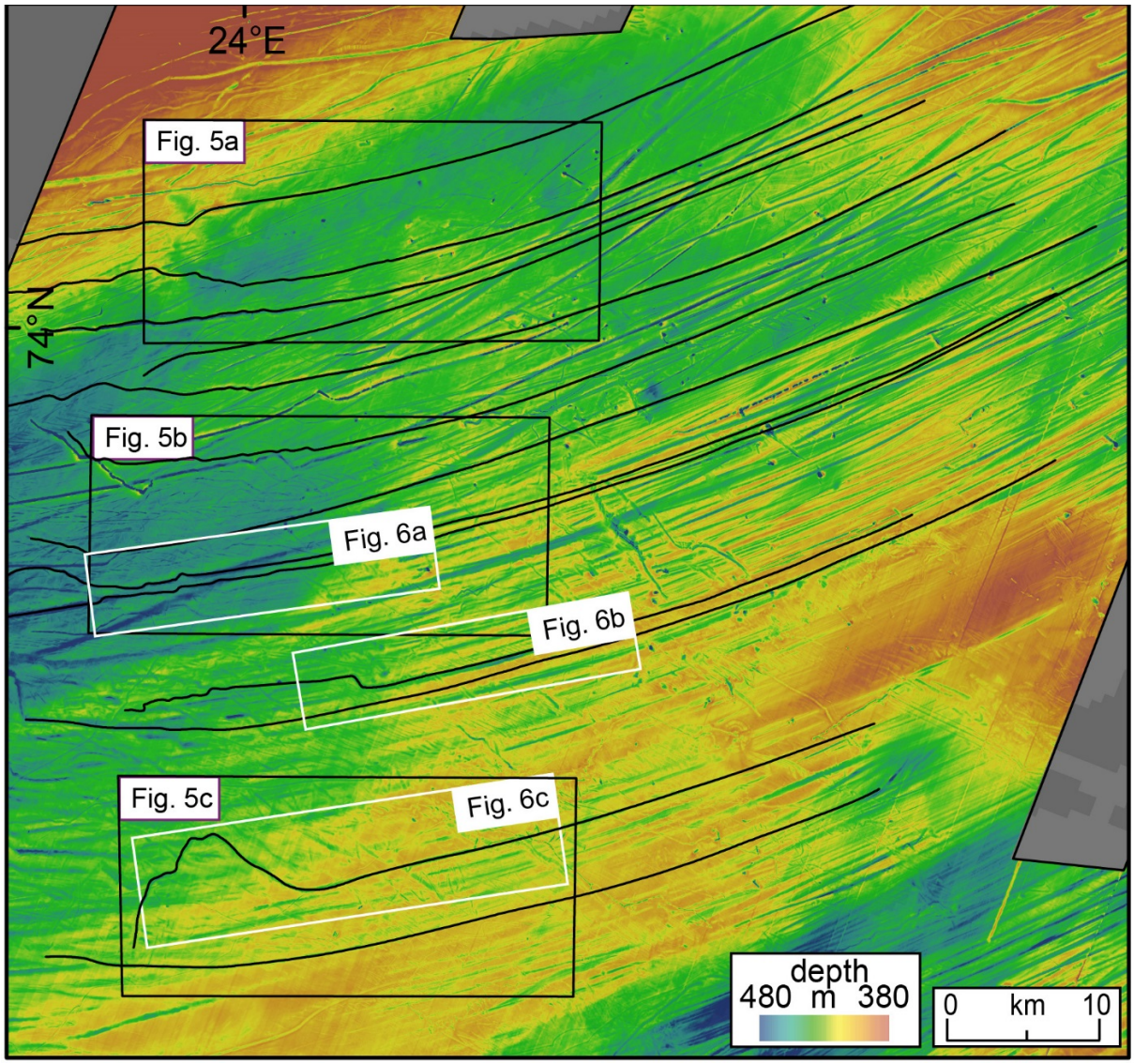
24°E
74°N
Fig. 5a
Fig. 5b
Fig. 6a
Fig. 6b
Fig. 5c
Fig. 6c
depth
480 m 380
0 km 10

822

823

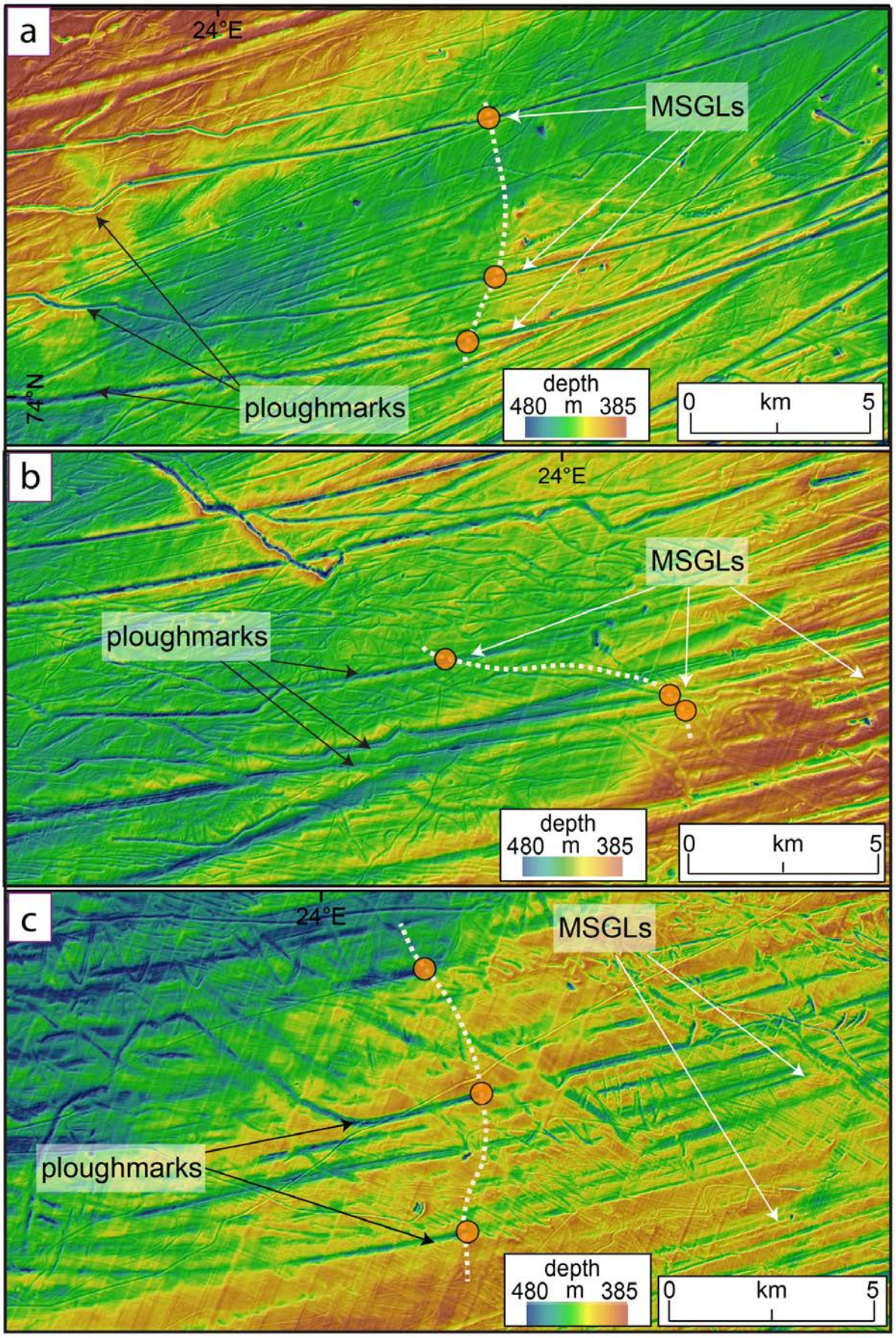
a
24°E
MSGLs
ploughmarks
74°N
depth
480 m 385
0 km 5
b
24°E
MSGLs
ploughmarks
depth
480 m 385
0 km 5
c
24°E
MSGLs
ploughmarks
depth
480 m 385
0 km 5

824

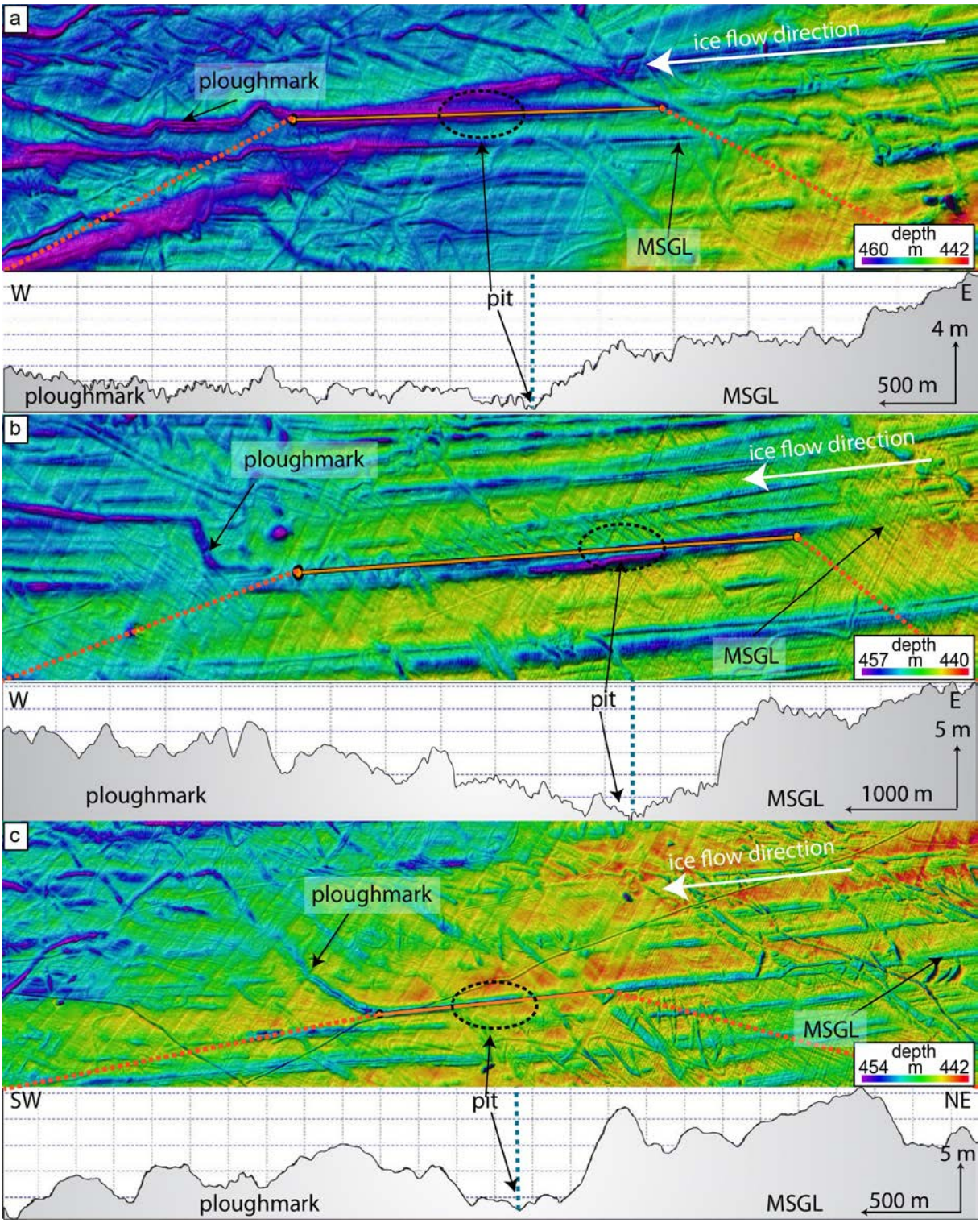
a
ploughmark
ice flow direction
MSGL
depth
460 m 442
W
E
pit
4 m
ploughmark
MSGL
500 m
b
ploughmark
ice flow direction
MSGL
depth
457 m 440
W
E
pit
5 m
ploughmark
MSGL
1000 m
c
ploughmark
ice flow direction
MSGL
depth
454 m 442
SW
NE
pit
5 m
ploughmark
MSGL
500 m

825

826

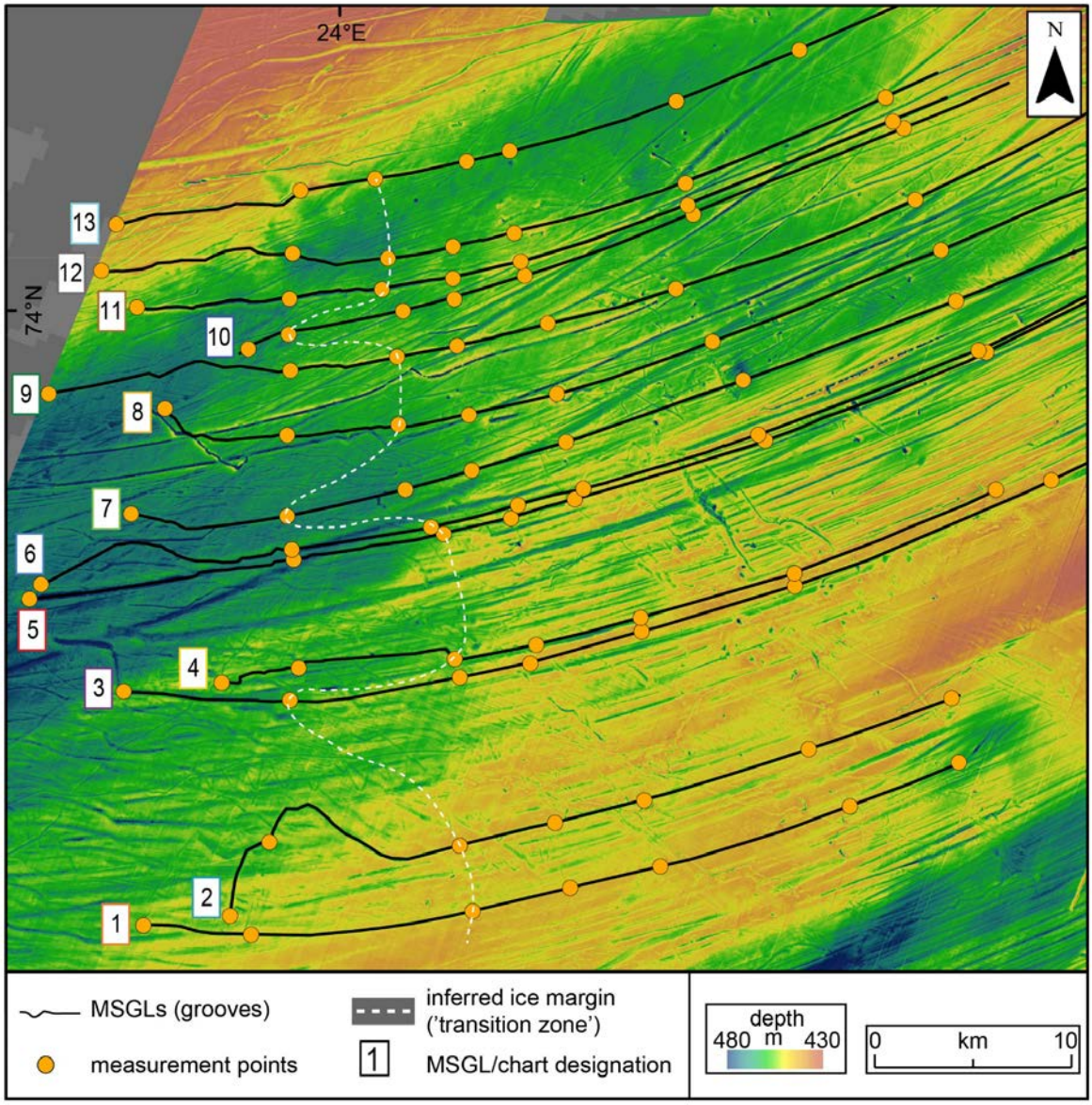
24°E
74°N
N
13
12
11
10
9
8
7
6
5
4
3
2
1
MSGLs (grooves)
measurement points
inferred ice margin
('transition zone')
1
MSGL/chart designation
depth
480 m 430
0 km 10

827

828

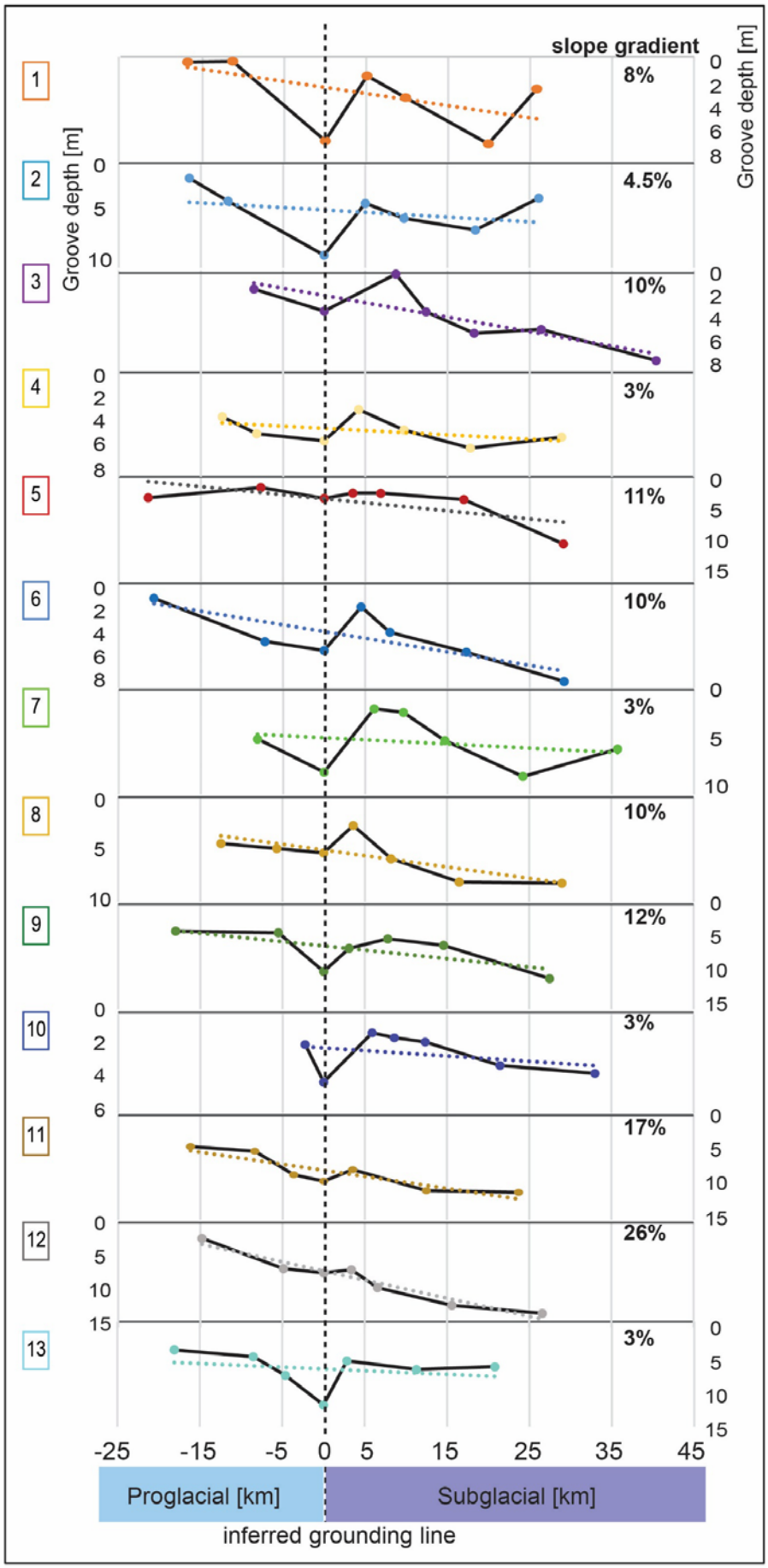
slope gradient
Groove depth [m]
Groove depth [m]
1
2
3
4
5
6
7
8
9
10
11
12
13
8%
4.5%
10%
3%
11%
10%
3%
10%
12%
3%
17%
26%
3%
-25
-15
-5
0
5
15
25
35
45
Proglacial [km]
Subglacial [km]
inferred grounding line

829

830

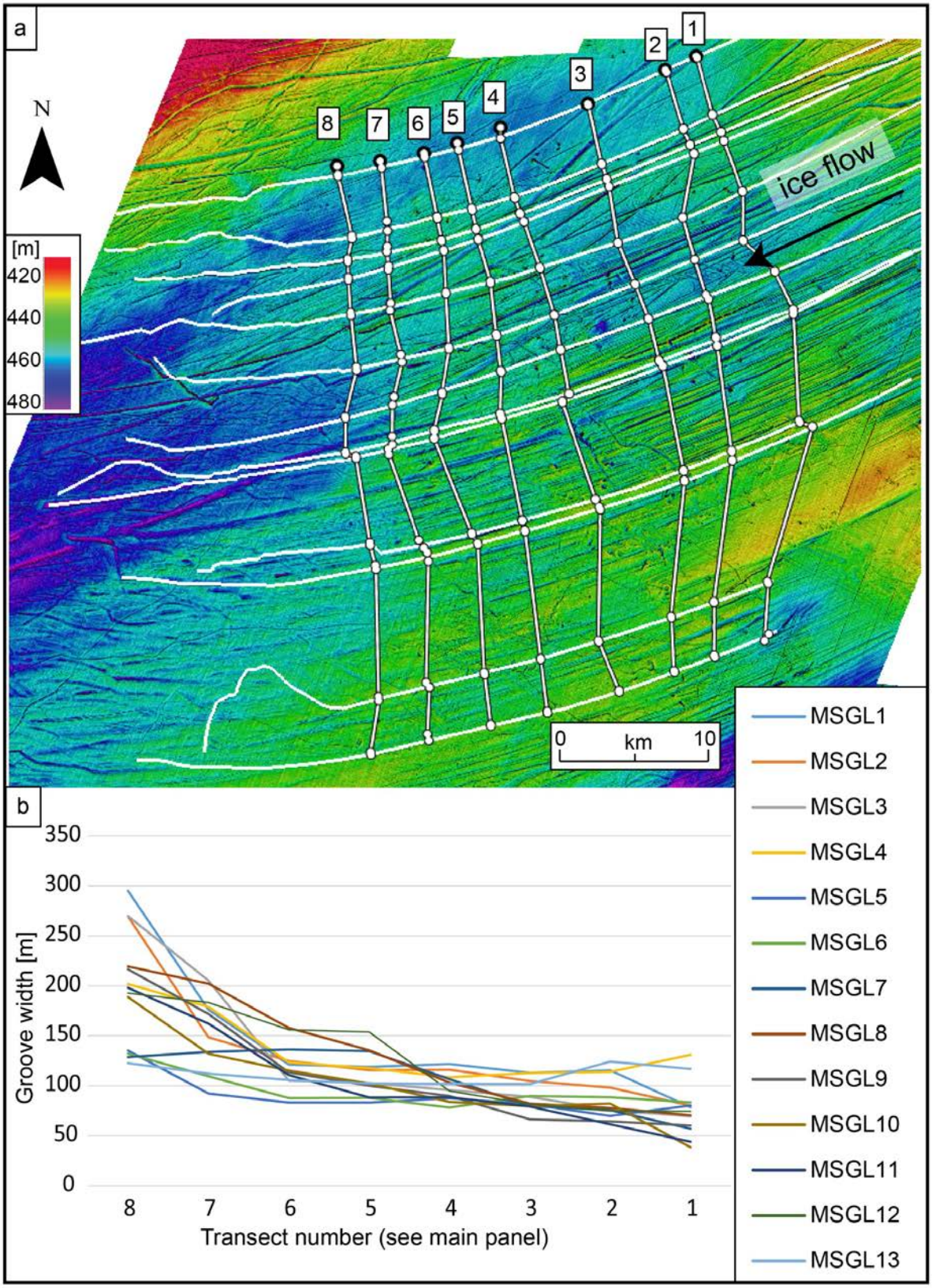
a
N
[m]
420
440
460
480
8
7
6
5
4
3
2
1
ice flow
0
km
10
b
Groove width [m]
350
300
250
200
150
100
50
0
8
7
6
5
4
3
2
1
Transect number (see main panel)
MSGL1
MSGL2
MSGL3
MSGL4
MSGL5
MSGL6
MSGL7
MSGL8
MSGL9
MSGL10
MSGL11
MSGL12
MSGL13

831

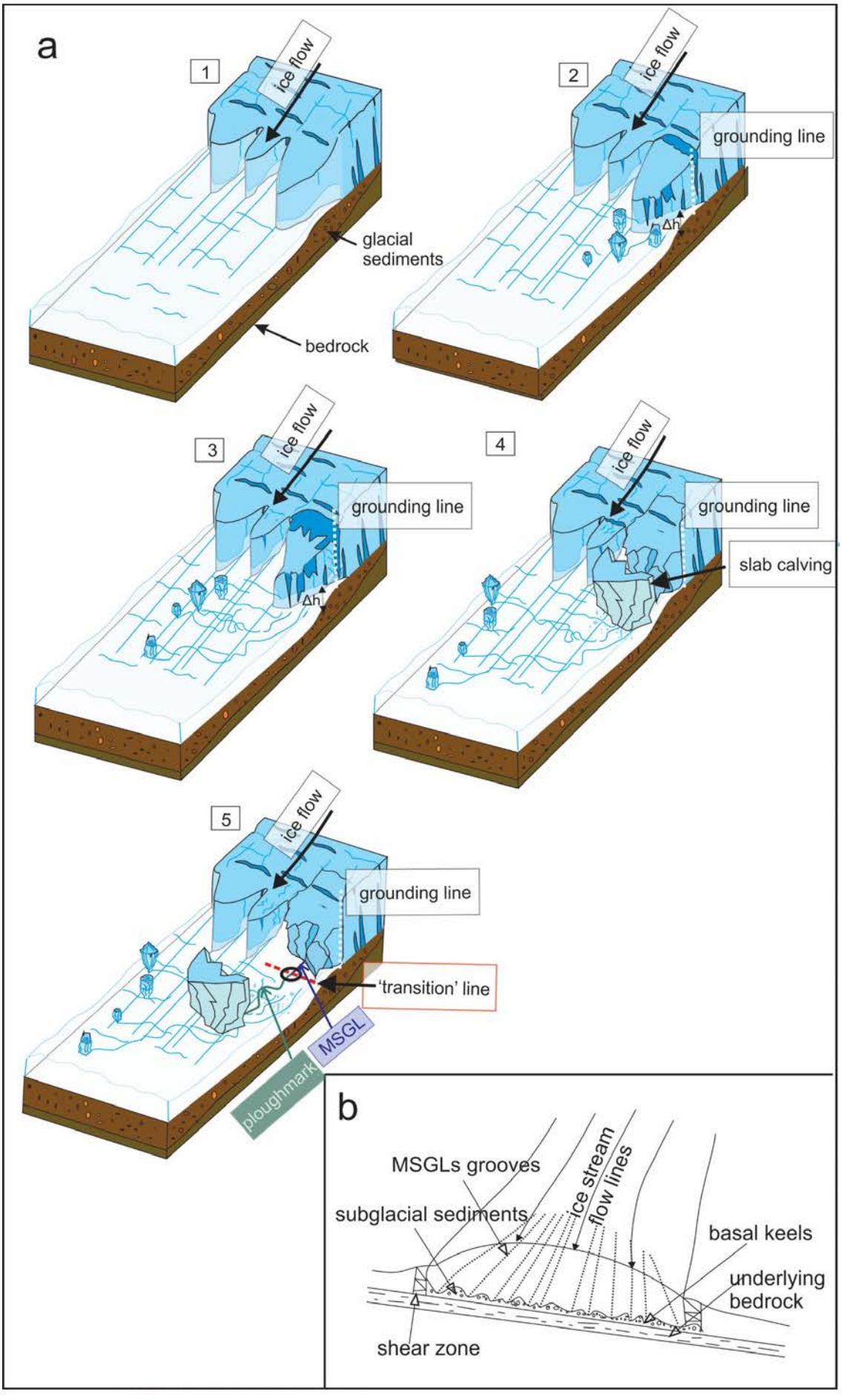
a
1
ice flow
glacial sediments
bedrock
2
ice flow
grounding line
Δh
3
ice flow
grounding line
Δh
4
ice flow
grounding line
slab calving
5
ice flow
grounding line
'transition' line
MSGL
ploughmark
b
MSGLs grooves
subglacial sediments
ice stream flow lines
basal keels
underlying bedrock
shear zone

832